Small-angle neutron scattering measurement of block copolymer interphase structure

Randal W. Richards and James L. Thomason*
Department of Pure and Applied Chemistry, University of Strathclyde, 295 Cathedral Street, Glasgow G1 1XL, UK
(*Received* 16 *November* 1982)

The notion of an interfacial layer at the domain boundary in block copolymers is reviewed and the possibility of its measurement by small-angle X-ray and small angle neutron scattering discussed. Values of the interfacial layer thickness and its volume fraction have been obtained for a range of styrene–isoprene copolymers. Interfacial layer thickness is not strongly dependent on molecular weight whilst the volume fraction shows a dependence more in line with the theory of Helfand.

Keywords Block copolymers; interphase; structure; neutron scattering; layer thickness

INTRODUCTION

Block copolymers of styrene (S) and isoprene (I) have a microphase separated solid state structure. The major features have been known for a number of years following the early application of transmission electron microscopy and small-angle X-ray scattering (SAXS) to their structural evaluation[1-6]. More sophisticated SAXS analyses have appeared recently together with some publications concerned with small angle neutron scattering (SANS) investigations[7-14]. All these studies show that these copolymers have a domain structure, the domain morphology being mainly determined by the composition of the copolymer. Typically domains have a diameter of ~100 to 300 Å whilst separation between domains is between approximately 300 to 1500 Å. Whilst there is a considerable degree of long range order between domains, it is clear that at larger length scales, 50–100 μm the copolymers have a mosaic structure. Relations between molecular weight, domain separation and domain size have been reported and discussed and a suitable theoretical description can be formed using a disordered macrocrystalline lattice as a basis[15].

Complementary to these experimental studies has been the development of statistical thermodynamic models of block copolymers. The first of these attempts is due to Meier[16-18] whilst the most highly developed at present is that of Helfand and Wasserman[19-23]. A different approach has been used by Leibler[24], who uses the random phase approximation of de Gennes to determine the phase diagram for these copolymers at the onset of microphase separation.

Apart from the gross features of domain size and separation, there has been much attention focussed on the domain boundary[18]. A region of finite thickness at the domain boundary, where the two copolymer components are mixed, has been invoked to account for the mechanical and dynamical behaviour of copolymers[25-29]. Positron annihalation results[30] clearly show the presence of a third phase coexisting with the pure domains and the matrix and which is identified as the interfacial region, or interphase, of finite thickness. The magnitude of this interphase has been a source of much theoretical effort and diametrically opposing ideas can be found. Thus Leary and Williams calculations[31,32] suggest that the interphase volume fraction approaches 0.5 whilst Krause[33] concludes that it must be no greater than 0.1. Meier[18] unifies apparently conflicting data in a model which has an interphase thickness increasing with decreasing molecular weight. This idea has been extended by Williams and co-workers[34] who also obtain considerable differences between copolymers with a diblock and those with a triblock architecture. By contrast, Helfand and coworkers[20-23] propose that the interphase has a thickness independent of molecular weight which is determined by the polymer step length and the interaction parameter of the polymers.

In view of this discussion and the attributed importance of the interphase, a paramount requirement is reliable values for the interphase thickness. The basis for its measurement using SAXS or SANS is discussed here together with the relative merits of the two techniques. Results are presented for a range of SI copolymers.

NATURE OF THE INTERPHASE

We provide a qualitative description of the interphase at domain boundaries, more detailed descriptions are available in the original papers[18,20-23,31-34]. The attainment of the minimum free energy in a microphase separated block copolymer system is achieved by balancing three contributions. In a copolymer with components A and B which are thermodynamically incompatible, the number of AB contacts can be reduced by decreasing the ratio of surface area to domain volume, this contribution therefore encourages growth. Opposing this growth mechanism, which is essentially enthalpic, is a need to maintain incompressibility in the system, i.e., the density

* Present address: Institut fur Physikalische Chemie, Universitat Mainz, D6500 Mainz, West Germany.

0032-3861/83/091089-08$03.00

within each phase should be uniform throughout. This is an essentially entropic limitation since it restricts chain conformations to those which fill space uniformly, i.e., extended conformations are favoured. Lastly, another entropic limitation to domain growth arises from the location of the junction between blocks to the domain boundary. This again reduces the conformational entropy. However, if the boundary is broadened by allowing A chains to wander into the B matrix over a finite range (and *vice versa*) the gain in entropy is larger than the contract free energy associated with AB contacts, thus reducing the overall free energy. It is this region which constitutes the interphase, a region where the density of phase A changes smoothly to that of phase B, and is characterized by an interphase thickness a_1. A variety of expressions have been used, mainly for empirical reasons, to describe the density profile, $\rho(r)$, across the interphase (linear, sinusoidal), the most theoretically sound equation[20-23] is:—

$$\rho(r)=0.5(1-\tanh(2r/a_1)) \quad (1)$$

with

$$a_1=(2/6^{0.5})b/x^{0.5} \quad (1a)$$

where b = Kuhn statistical step length and X = polymer–polymer interaction parameter. The form of $\rho(r)$ defined by equation (1) is shown in *Figure 1*.

MEASUREMENT OF INTERPHASE THICKNESS

The small-angle scattering envelope from block copolymers can be divided into three regions; at the very low angles i.e., scattering vectors, Q, $< \sim 0.04$ Å^{-1}, it is dominated by Bragg scattering due to the interference function; at somewhat higher angles features due to single particle form factor scattering are dominant; finally for scattering vectors wherein $QR \gg 1$ for all dimensions, R, of the particle, the Porod region is explored[12,14]. It is this latter region which is utilized in the measurement of interphase thickness, the other regions have been discussed elsewhere.

In the Porod region and for particles of arbitrary shape and sharp boundaries but random orientation with respect to the incident wave vector, then the scattered intensity is described by Porods law[35,36].

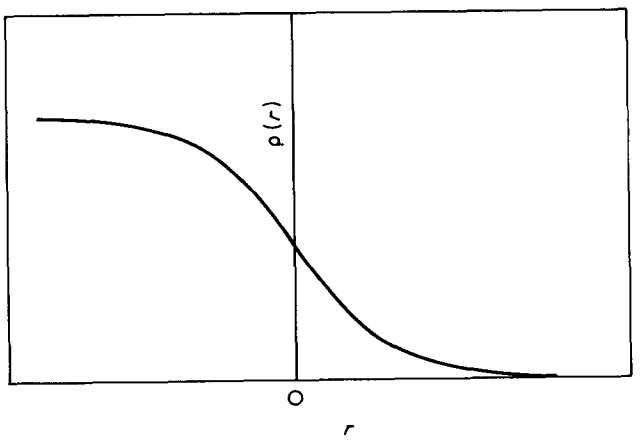

Figure 1 Density variation across the interface according to equation (1)

$$I(Q)=K2\pi(A_p/V_p^2)Q^{-4} \quad (2)$$

where K is a collection of instrumental and calibration factors, A_p and V_p are the particle surface area and volume respectively. Ruland[37] has related deviations from this law to positive and negative contributions to the scattered intensity. Positive contributions in the scattering from solid polymers have been attributed to void scattering and scattering due to thermal density fluctuations[38]. Together these constitute an addition to equation (2), since this type of scattering may depend on the scattering vector, we write this contribution as a Q dependent background $I_B(Q)$, thus

$$I(Q)=K(S\pi(A_p/V_p^2)Q^{-4}+I_B(Q) \quad (3)$$

Negative contributions arise from a diffuse boundary at the particle–matrix interface. Boundaries of finite width can be introduced by smoothing the edges of the density distribution in one ideal two phase system by convolution with a smoothing function, $h(r)$[37]. In terms of equation (3) this results in:

$$I(Q)=K(2\pi(A_p/V_p^2)Q^{-4}.H^2(Q)+I_B(Q)) \quad (4)$$

where $H^2(Q)$ is the Fourier transform of $h(r)$. Consequently, the determination of the interphase thickness from scattering data resolves into two problems, firstly the subtraction of the background scattering $I_B(Q)$, secondly the use of a suitable form for $H^2(Q)$ which is related to the density profile across the interphase.

In SAXS the major source of background scattering in the Porod region is the thermal density fluctuation. This background scattering has been subtracted using empirical functions obtained by fitting to scattering data in a somewhat higher Q region and extrapolating into the Porod region[39]. It has been demonstrated by Roe[44] that the use of the wrong empirical function for the background intensity can lead to grossly erroneous values of the interphase thickness. For the case of SANS, there is an additional contribution to the background, the incoherent scattering. Small-angle neutron scattering from phase separated polymer systems has recently been discussed by Koberstein[40], following Ruland's analysis the background scattering is written as

$$I_B(Q)=I_B(0)\exp(DQ^2/I_B(0)) \quad (5)$$

D in equation (5) is determined by empirical fitting, as in SAXS, in a phase separated system.

$$I_B(0)=\rho_1\phi_1\sigma_1+\rho_2\phi_2\sigma_2 + \phi_1a_1^2\rho_1^2kT\kappa_1+\phi_2a_2^2\rho_2^2kT\kappa_2 \quad (6)$$

where ρ_i = number density of monomer i
σ_i = incoherent scattering cross section
a_i = coherent scattering length
κ_i = isothermal compressibility.

Calculations show that the incoherent scattering contributions to equation (6) are ~ 400 times the thermal

density fluctuations (κ_i terms) in equation (6). Consequently the exponential term in equation (3) becomes negligible and hence it is expected that the background scattering in SANS should be flat and isotropic making extrapolation to lower regions of Q much easier.

The form of $H(Q)$ is defined by the choice of $h(r)$, the smoothing function which is defined so that its convolution with an ideal step boundary will produce a profile identical to the density profile across the interphase. For a density profile of equation (1), Ruland[41] has derived:—

$$h(r)=1/a_1\cosh^2(2r/a_1) \tag{7}$$

whence

$$H(Q)=\frac{\pi a_1 Q}{4\sinh(0.25\,a_1 Q)} \tag{8}$$

Using equation (8) in the analysis of scattering data makes extraction of a_1 difficult, recourse has been made to the simpler approximation of a Gaussian distribution[39,41] for the smoothing function:

$$h(r)=\frac{1}{(2\pi\sigma^2)^{0.5}}\exp(-r^2/2\sigma^2) \tag{9}$$

whence

$$H(Q)=\exp(-\sigma^2Q^2/2) \tag{10}$$

The forms of equations (7) to (10) are shown in *Figure 2*.

Helfand[23] has suggested that the extent of $H(Q)$ available to small-angle scattering techniques is such that only the second moment of the density variation is measurable. Thus if the original Gaussian distribution is retained then the interphase thickness, t, is:—

$$t=12^{0.5}\sigma \tag{11}$$

whereas if the notion that σ^2 is the second moment of the density variation then:—

$$\sigma=a_1\pi/4.6^{0.5} \tag{12}$$

In the Porod region for a particle with diffuse boundaries the scattered intensity after subtraction of background is obtained by combining equations (4) and (10) as,

$$I(Q)=K2\pi(A_p/V_p^2)Q^{-4}\exp(-\sigma^2Q^2) \tag{13}$$

whence

$$\ln(Q^4I(Q))=\ln(K2\pi A_p/V_p^2)-\sigma^2Q^2 \tag{14}$$

and σ^2 is then easily obtained from the slope of a plot of the left hand side as a function of Q^2.

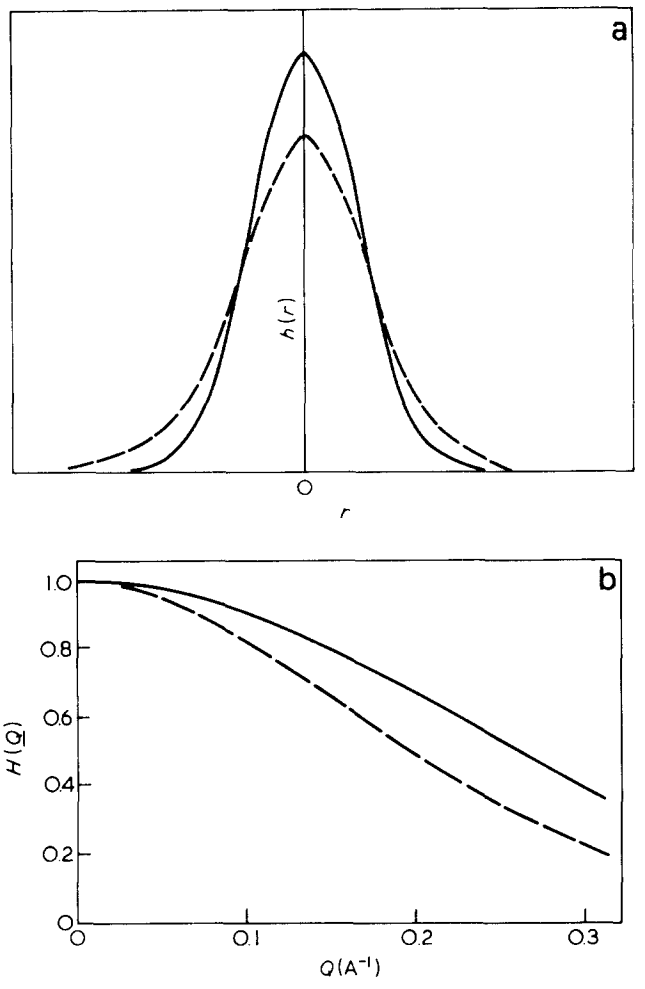

Figure 2 (a) Smoothing functions, $h(r)$, as a function of r. (———) Gaussian; (– – –) Ruland's equation. (b) Fourier transform of the smoothing functions in *Figure 2a*

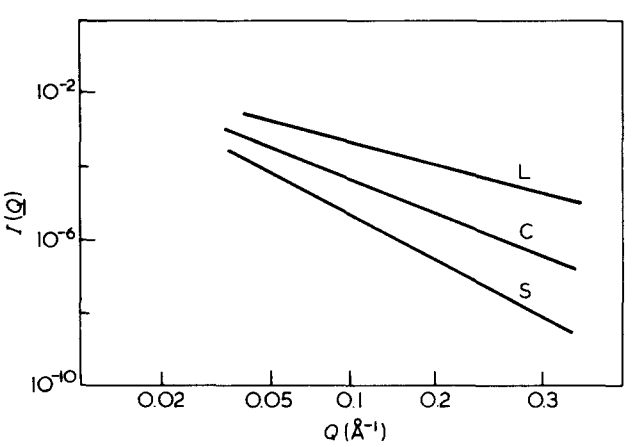

Figure 3 Asymptotic scattered intensity calculated for lamellar, L, cylindrical, C, and spherical, S, particles. Dimensions of particles used in calculations are: $R_s=R_c=200$ Å, $L=400$ Å. Slopes of lines are: line L = −2, line C = −3, line S = −4

DOMAIN MORPHOLOGY AND INTERPHASE MEASUREMENT

All the foregoing comments apply to particles with random orientation, however, for block copolymers with lamellar and cylindrical domain morphology this is not the case. The mosaic structure has a random spread of orientations but within each 'mosaic unit' the domains are reasonably well ordered[14,15]. Because the spread in mosaic orientation (~180°) is much greater than the beam divergence (~1°), only those domains which satisfy the Bragg condition will contribute to the scattering envelope[42]. Those domains which do not satisfy this condition will only contribute to the incoherent background scattering. To encompass this situation, rather

than use a Porod law we have to use the convolution of the single particle form factor for the domain with $H^2(Q)$. Single particle form factors in the intermediate Q range are shown in *Figure 3*, the analytical expression in this Q region being given by:—

Sphere

$$\langle F_p(Q)\rangle^2 = 2\pi(A_p/V_p^2)Q^{-4} \quad (15)$$

for $Q > 2\pi/R$;

Cylinder

$$\langle F_p(Q)\rangle^2 = 4/\pi Q^3 R_c^3 = (2/\pi R_c^2)(A_p/V_p)Q^{-3} \quad (16)$$

for $Q > 2\pi/R_c$, where R_c = cylinder radius;

Lamellae

$$\langle F_p(Q)\rangle^2 = 2Q^{-2}/L^2 = (1/L)(A_p/V_p)Q^{-2} \quad (17)$$

for $Q > 2\pi/L$, where L = lamella thickness.
Using this procedure then for spherical domains the equation obtained is identical to equation (13). For cylindrical domains we obtain:

$$I(Q) = K(2/\pi R_c^2)(A_p/V_p)Q^{-3}H^2(Q) \quad (18)$$

whence

$$\ln(Q^3 I(Q)) = \ln(2KA_p/\pi R_c^2 V_p) - \sigma^2 Q^2 \quad (19)$$

For lamellar domains this procedure produces:

$$I(Q) = K(1/L)(A_p/V_p)Q^{-2}H^2(Q) \quad (20)$$

yielding

$$\ln(Q^2 I(Q)) = \ln(KA_p/LV_p) - \sigma^2 Q^2 \quad (21)$$

COMPARISON OF SAXS AND SANS FOR MEASUREMENT OF INTERPHASE THICKNESS

The equations set out above for the analysis of scattering in the Porod region are applicable directly only when the radiation source has point collimation. For many SAXS instruments this is not the case, the source generally being slit like. Desmearing of the data can produce artefacts and attempts have been made to develop equations suitable for smeared data and some success reported in using such a full analysis[7,8]. This problem is avoided in SANS since neutron diffractometers have point source collimation.

A possible source of error in SAXS may be the subtraction of the background. The background scattering in SAXS arises from thermal density fluctuations and it is estimated by fitting to the scattering curve in the wide angle region. Whilst the validity of the subsequent extrapolation into the Porod region is not questioned, the empirical functions used for the fitting may be a cause of some uncertainty. As we have seen, in SANS the major contribution to the background is the incoherent scattering signal. Although its magnitude relative to that due to interphase scattering may be larger than that of the thermal density fluctuation in SAXS, the fact that it is flat and isotropic greatly simplifies its subtraction over the relevant region of scattering vector.

All radiation scattering techniques respond to density fluctuations in the material being investigated. Consequently to improve signal to noise ratios these fluctuations should be as large as possible. SAXS responds to electron density fluctuations whilst SANS responds to scattering length density variation in the specimen. For most organic materials electron densities are fairly similar as are the scattering length densities for protonated substances. However, if one component is selectively deuterated the scattering length density is dramatically changed without significantly influencing the thermodynamic properties of the specimen. *Figure 4* shows the change in magnitude of the relevant density function for SAXS and SANS from SI copolymers. Clearly, the difference for the part deuterated copolymer is much greater than for the other two examples. Consequently, the combination of SANS with a part deuterated copolymer would appear to be a much more favourable situation for the determination of the interphase thickness.

EXPERIMENTAL

Copolymer preparation

Styrene–isoprene block copolymers with deuterated styrene blocks were prepared by anionic polymerization,

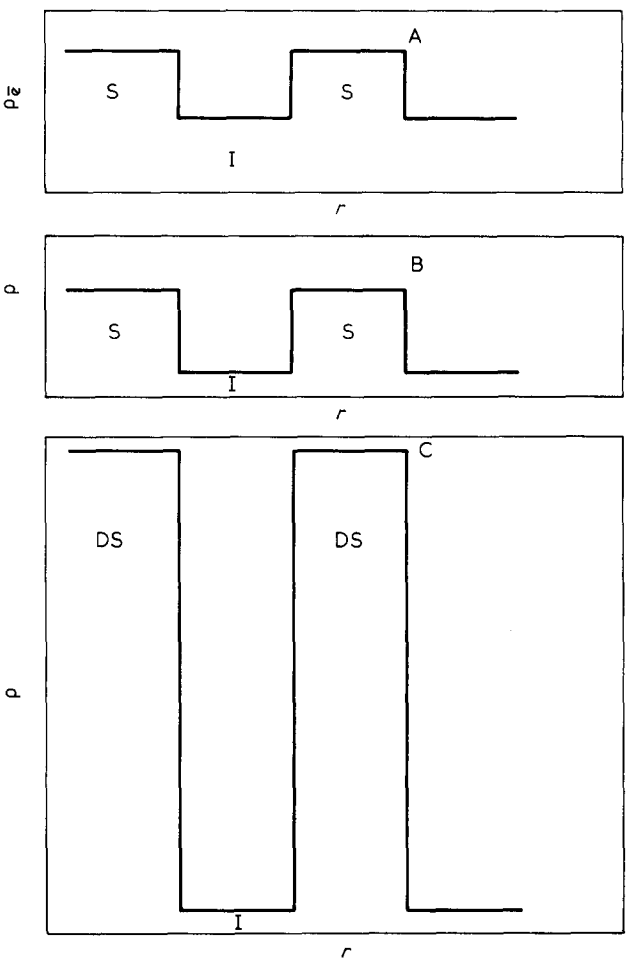

Figure 4 Schematic diagram of relative variation in electron density, $\rho_{\tilde{e}}$, and scattering length density, ρ, for styrene and isoprene units

the details of which were published earlier[13,14]. The compositions were determined by u.v. spectrometry using chloroform solutions whilst molecular weights were measured by gel permeation chromatography subsequently corrected by a procedure outlined earlier. *Table 1* sets out the characteristics of the copolymers investigated here.

Small-angle neutron scattering

Samples for SANS were cast from 8% (w/v) copolymer solutions in toluene onto optical quality quartz discs which were used as sample supports. Typically, specimens were 0.5 to 1 mm thick but some specimens were made with thicknesses as low as 0.1 mm to assess the influence of multiple coherent scattering especially in those copolymers with more than 30% w/w deuterated styrene. No evidence for multiple scattering was observed. For the purpose of determining the interphase thickness, scattering envelopes in the intermediate Q range were obtained using the D17 diffractometer at the Institut Laue-Langevin, Grenoble, France and the small angle spectrometer at AERE Harwell, UK. The data were corrected for scattering from the quartz support and normalized to the scattering from a 2 mm thick water specimen using analysis procedures developed by Dr R. E. Ghosh[43]. The regrouped data was then transferred to the central computer at the University of Strathclyde where all subsequent data analysis was performed.

RESULTS

Typical scattering envelopes for each morphology are shown in *Figure 5* over the total Q range in which these copolymers were investigated. These figures were obtained by combining data from different Q ranges which have been discussed in an earlier publication[14]. For low Q (<0.04 Å^{-1}) the 'Bragg' scattering is observable as a series of discrete peaks, at higher Q weak oscillations become evident due to single particle form factor scattering. Eventually for $Q>0.2$ Å^{-1}, the scattered intensity becomes a constant value. This constant scattered intensity at $Q>0.2$ Å^{-1} has been used as the value of the incoherent background scattering and subtracted from the data at $Q<0.2$ Å^{-1} preparatory to further analysis by equations (14), (19) or (21). *Figure 6* shows data for a copolymer with spherical domains analysed according to equation (14), for $Q>0.07$ Å^{-1} a line of negative slope is evident. From a least squares straight line drawn through data over the range $0.07<Q<0.15$ a value of σ^2 has been calculated. By comparison, the same type of plot for the equivalent hydrogenous copolymer is shown in *Figure 7*. Due to the small difference in scattering length density between hydrogenous styrene and isoprene the signal to noise ratio is much lower and the data is widely scattered with no clear trend. Interphase thicknesses, t, were calculated from equation (11) and are given in *Table 2* together with σ^2 for each copolymer.

Similar analyses were used for copolymers with cylindrical and lamellar morphology using the analysis appropriate to their morphology (equations (19) and (21)). *Figures 8* and *9* show typical plots for these two morphologies whilst *Figure 9* also shows the plot that is obtained if no account is taken of domain morphology and orientation for a lamellar morphology copolymer. *Tables 3* and *4* give values of σ^2 and t calculated from least squares lines through the relevant data points.

Table 1 Characterization data for copolymers investigated

Sample	$10^{-3}\bar{M}_n$	$\bar{M}_w/\bar{M}_n$	W_s
DSI1	62.18	1.06	0.329
DSIS1	46.12	1.08	0.122
DSIS2	68.67	1.07	0.340
ABC1	86.00	1.06	0.212
DSI3	114.08	1.58	0.398
DSI5	99.57	1.34	0.817
DSI6	132.43	1.49	0.545
DSI10	81.21	1.29	0.428
DSI7	16.72	1.50	0.482
DSI9	32.63	1.61	0.579
DSI11	59.33	1.09	0.531

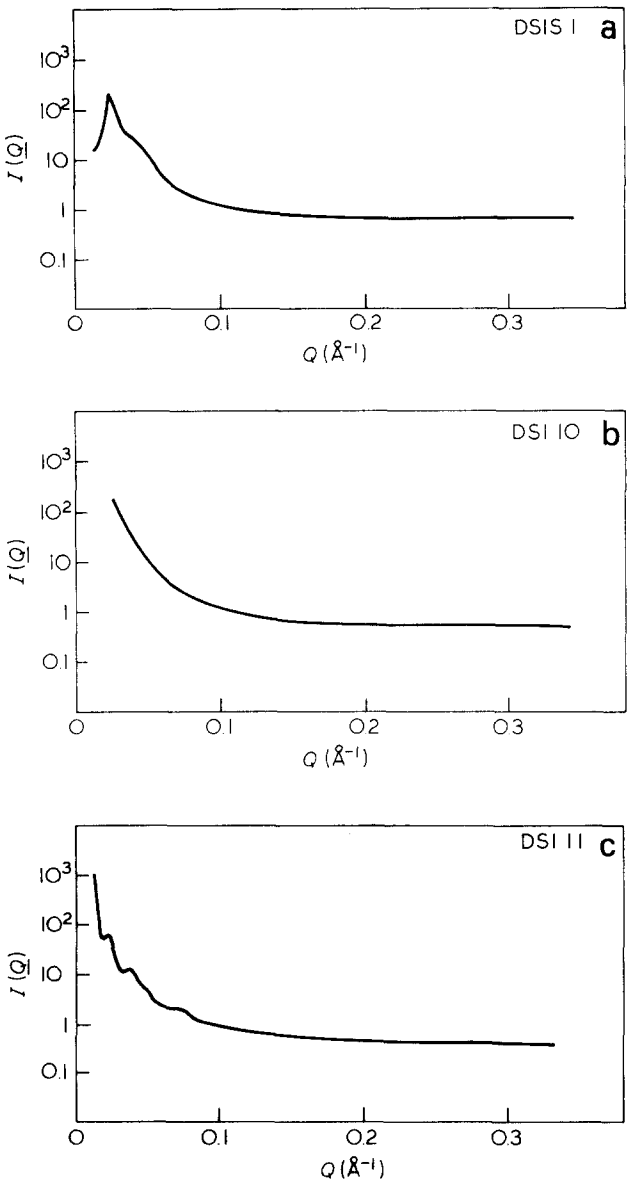

Figure 5 Typical SANS scattering envelopes for (a) spherical, (b) cylindrical and (c) lamellar domains

DISCUSSION

Since the nature of the interphase in block copolymers is primarily determined by local interactions[16-23], a dependence of interphase thickness on copolymer com-

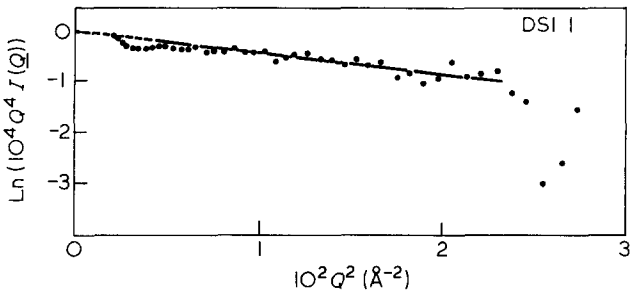

Figure 6 Plot of data according to equation (14) for copolymer DSI1

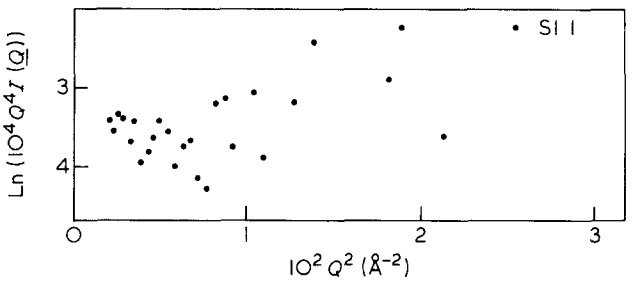

Figure 7 Data for a hydrogenous copolymer plotted according to equation (14)

Table 2 Interphase characteristics for spherical domains

Sample	σ^2 (Å^2)	t (Å)
DSI1	47	23.7
DSIS1	123	38.5
DSIS2	39	21.6
ABC1	49	24.3

position is not to be expected. This expectation is borne out by the results obtained here since there is clearly no discernable trend in the values of t with composition. A semi-logarithmic plot of t as a function of copolymer molecular weight is shown in *Figure 10*. Values calculated from theory are shown for comparison using the predictions of Williams and co-workers[34], Meier[18] and Helfand[19-23]. For the latter theory, t has been calculated using the relation

$$t = \pi a_1 / 2.828$$

a_1 being calculated from equation (1a). Apart from one anomalously high value, our data mainly lies around the value predicted from Helfand's theory, an average experimental value of 21.6 Å being obtained compared with a theoretical prediction of 15.6 Å. Similar values of t for lamellar and spherical copolymers have been obtained by Hashimoto[7,8] using SAXS. The theoretical values of t from Williams *et al.*, and Meier's theories appear to be far too large, in particular there seems to be no evidence for a maximum in t, however this maximum is not of sufficient magnitude to be distinguishable from the experimental uncertainty in t.

Whilst the correlation of interphase thickness with various theoretical predictions is necessary to discern between them, the more important parameter, from the point of view of mechanical properties, is the volume fraction of the interphase, ΔV_I, in the copolymer system. Calculation of this parameter necessitates a knowledge of the domain separation, d_{int}, and domain size. Values for these quantities for the copolymers investigated here have been reported in an earlier publication[14]. For lamellar morphology copolymers, ΔV_I was calculated from:

$$\Delta V_I = 2t/d_{int} \tag{22}$$

whilst for cylindrical domains which adopt a hexagonally close packed structure then:

$$\Delta V_I = 2\pi/3^{0.5}[(R_1/d_{int})^2 - (R_2/d_{int})^2] \tag{23}$$

where $R_1 = R_c + t/2$
$R_2 = R_c - t/2$

For spherical domains there is some uncertainty over the

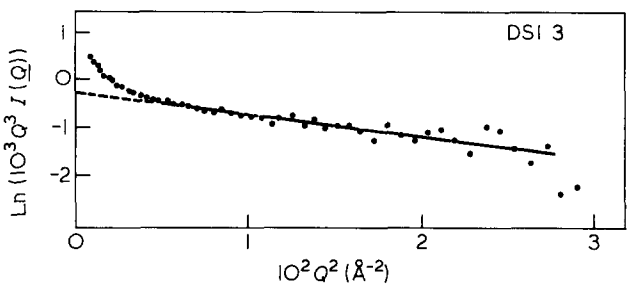

Figure 8 Data for copolymer DSI3 plotted according to equation (19)

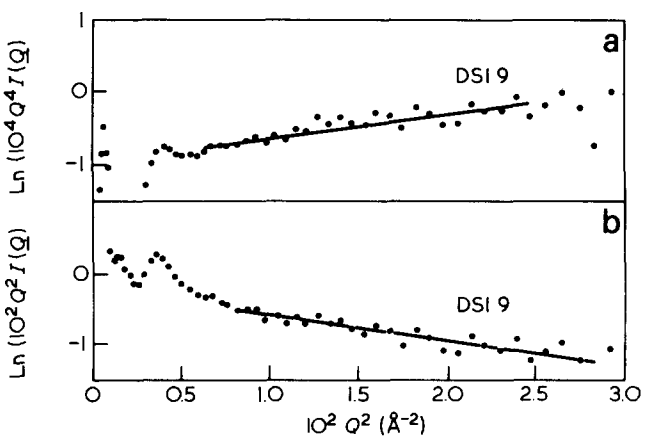

Figure 9 Data for copolymer DSI9 plotted (a) according to equation (14); (b) according to equation (21)

Table 3 Interphase characteristics for domains

Sample	σ^2 (Å^2)	t (Å)
DSI7	40	22
DSI9	37	21
DSI11	27	18

Table 4 Interphase characteristics for cylindrical domains

Sample	σ^2 (Å^2)	t (Å)
DSI3	44	23
DSI5	21	16
DSI6	12	12
DSI10	27	18

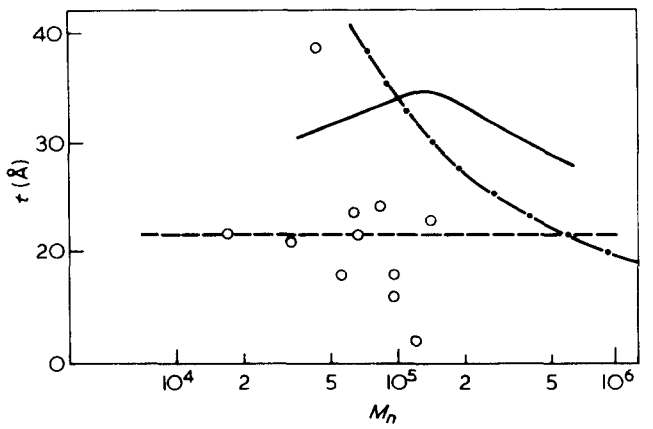

Figure 10 Interphase thickness of deuterated copolymers: (○) experimental values; (---) Helfand narrow interphase approximation value; (-·-·-) obtained from Meier's theory; (———) calculated by Williams and co-workers

precise arrangement of domains with respect to each other. A cubic arrangement gives the best agreement with experimental results, whilst a simple cubic structure is in no way suitable, it is not possible to differentiate between a body centred cubic or a face centred cubic arrangement of spheres. For the three possible arrangements then:

Simple cubic

$$\Delta V_I = 4\pi/3((R_1/d_{int})^3 - (R_2/d_{int})^3) \quad (24)$$

Body centred cubic

$$\Delta V_I = 3^{0.5}\pi((R_1/d_{int})^3 - (R_2/d_{int})^3) \quad (25)$$

Face centred cubic

$$\Delta V_I = (8.\pi/2^{0.5} \times 3)((R_1/d_{int})^3 - (R_2/d_{int})^3) \quad (26)$$

The difference in ΔV_I calculated by equation (25) or (26) is less than 10%, a value which is within experimental error, consequently we are unable to differentiate between the structures from a comparison of ΔV_I values with theoretically calculated quantities. *Figure 11* is a semi-logarithmic plot of ΔV_I as a function of molecular weight, calculated using equations (22), (23) and (25) or (26) using experimental values of t obtained in this work. Additional data required, e.g. d_{int} and domain sizes were obtained from SANS data reported earlier. Theoretical values have been calculated from Helfand's theory using an interphase thickness of 22 Å which is compatible with $a_I = 14$ Å, Meier's values of ΔV_I are also included for comparison. Helfand's theory of the interphase gives better agreement with the experimental data, the lower experimental values of ΔV_I are attributable to the experimental domain separations being larger than the comparable theoretical values[14].

Referring back to the analysis used for spherical domains, equation (14), then the intercept is:

$$\text{Intercept} = \ln(K 2\pi A_p/V_p^2)$$

It can be shown that the factor K is given by[12]

$$K = 4\pi D_s T_s K_f \phi_p V_p/(1 - T_w)$$

where

D_s = sample thickness

T_s = neutron transmission factor for sample

T_w = neutron transmission factor for water calibrant

ϕ_p = volume fraction of domain

$K_f = (\rho_s - \rho_I)^2$

with ρ_s = coherent scattering length of deuterostyrene

ρ_I = coherent scattering length of isoprene.

The product of $(A_p/V_p^2)V_p$ for a spherical domain is $(3/R_s)$. Consequently from the intercepts of the plots for spherical domains a value for the domain size can be calculated. This provides a check on the analysis, since values of R_s can be compared with values obtained directly from the single particle form factor scattering. *Table 5* sets out values of spherical domain radius obtained in this way together with values obtained directly[14]. For most of the copolymers the agreement between the two techniques is excellent. The poor agreement for DSIS2 may be due to the presence of some cylindrical domains, since its composition is such that it approaches a region wherein cylindrical structures are the more stable morphology, however earlier analysis is more in agreement with a spherical structure. This type of analysis cannot be used for lamellar and cylindrical domains because evaluation of the intercept terms results in the area of the domain remaining as a discrete quantity which cannot be simplified further. Additionally, due to the necessity to fulfill the Bragg condition, evaluation of this term requires a knowledge of the number of domains which are correctly aligned. Unfortunately, this number is not calculable.

ACKNOWLEDGEMENTS

We thank the Science and Engineering Research Council for financial support of this research. Dr H. Hässlin at ILL and Mr V. Rainey at AERE Harwell are thanked for their technical assistance. Dr R. J. Whewell's assistance in the preparation of the manuscript was invaluable.

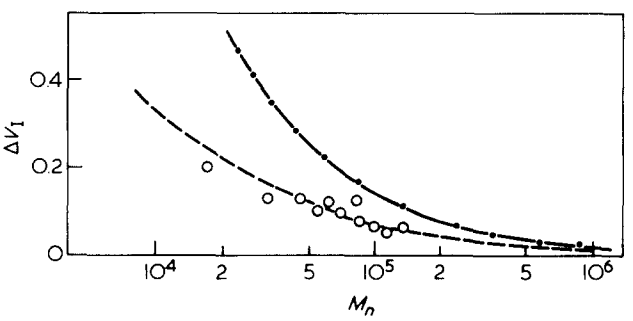

Figure 11 Interphase volume fraction obtained from SANS data (○): (---) calculated from Helfand's theory; (-·-·-) calculated from Meier's theory

Table 5 Domain size for spherical domains obtained from equation (14)

Sample	Domain radius (Å)	
	From intercept of equation (14)	From SPFF
DSI1	153	173
DSIS1	72	73
DSIS2	40	190
ABC1	162	175

APPENDIX

Analytical expressions for the single particle form factor at high Q

Lamellar domains.

$$\langle F_p(Q)\rangle^2 = (\pi/2x)J_{1/2}^2(x)$$

where $x = QL/2$

therefore

$$\langle F_p(Q)\rangle^2 = \sin^2(x)/x^2.$$

Since

$$\overline{\sin^2(x)} = 0.5,$$

then

$$\langle F_p(Q)\rangle^2 = 2/Q^2L^2 = 1/L)(A_p/V_p)Q^{-2}$$

Cylindrical domains.

$$\langle F_p(Q)\rangle^2 = 4J_1^2(x)/x^2$$

where $x = QR_c$. For large x,

$$\langle F_p(Q)\rangle^2 = (8/\pi x^3)(A(x)\cos(x^*) - B(x)\sin(x^*))^2$$

where $x^* = x - 3\pi/4$.

$$A(x) \simeq 1 + \frac{15}{2!(8x)^2} - \frac{14175}{4!(8x)^4} + \ldots..$$

$$B(x) \simeq \frac{3}{8x} - \frac{315}{3!(8x)^3} + \frac{1090000}{5!(8x)^5} - \ldots..$$

$$\langle F_p(Q)\rangle^2 = (8/\pi X^3)(A^2(x)\cos^2(x^*) + B^2(x)\sin^2(x^*) - 2AB\cos(x^*)\sin(x^*))$$

Since $\overline{\sin^2(x^*)} = \overline{\cos^2(x^*)} = 0.5$ and $\overline{\cos(x^*)\sin(x^*)} = 0$ then

$$\langle F_p(Q)\rangle^2 = (4/\pi x^3)(A^2(x) + B^2(x))$$
$$= (4/\pi x^3)(1 + 0.375/x^2 - 0.351/x^4)$$

For large x this tends to

$$\langle F_p(Q)\rangle^2 = 4/\pi x^3 = (2/\pi R_c^2)(A_p/V_p)Q^{-3}$$

Spherical domains.

$$\langle F_p(Q)\rangle^2 = (9\pi/2x^3)J_{3/2}^2(x)$$

where $x = QR_s$

$$\langle F_p(Q)\rangle^2 = (9/x^6)(\sin(x) - x\cos(x))^2$$
$$= (9/2)(1/x^4 + 1/x^6)$$

For large x,

$$\langle F_p(Q)\rangle^2 = 9/2x^4 = (2\pi/((4/3)\pi R_s^3))(3/R_sQ^4)$$
$$= (2\pi/V_p)(A_p/V_p)Q^{-4}$$

REFERENCES

1 Holden, G., Bishop, E. and Legge, N. *J. Polym. Sci.*, (C) 1969, **26**, 59
2 Gallot, B. R. M. *Adv. Polym. Sci.* 1978, **29**, 85
3 Lewis, P. R. and Price, C. *Polymer* 1971, **12**, 258
4 Lewis, P. R. and Price, C. *Polymer* 1972, **13**, 20
5 McIntyre, D. and Campos-Lopez, E. *Macromolecules* 1970, **3**, 322
6 Legrand, A. D., Vitale, G. G. and Legrand, D. G. *Polym. Eng. Sci.* 1977, **17**, 598
7 Hashimoto, T., Shiboyama, M. and Kawai, H. *Macromolecules* 1980, **13**, 1237
8 Hashimoto, T., Fujimura, M. and Kawai, H. *Macromolecules* 1980, **13**, 1660
9 Hadziioannou, G., Picot, C., Skoulios, A., Ionescu, M-L., Mathis, A., Duplessix, R., Gallot, Y. and Lingelser, J. P. *Macromolecules* 1982, **15**, 263
10 Bates, F. S., Cohen, R. E. and Berney, C. V. *Macromolecules* 1982, **15**, 589
11 Berney, C. V., Cohen, R. E. and Bates, F. S. *Polymer* 1982, **23**, 1222
12 (a) Richards, R. W. and Thomason, J. L. *Polymer* 1981, **22**, 581; (b) Jacrot, B. and Zaccai, G. *Biopolymers* 1981, **20**, 2413
13 Richards, R. W. and Thomason, J. L. *Polymer* 1983, **24**, 275
14 Richards, R. W. and Thomason, J. L. *Macromolecules* (In Press)
15 Richards, R. W. and Thomason, J. L. manuscript in preparation
16 Meier, D. J. *J. Polym. Sci.* (C) 1969, **26**, 81
17 Meier, D. J. *Polym. Prepr.* 1970, **11**, 400
18 Meier, D. J. *Polym. Prepr.* 1974, **15**, 171
10 Helfand, E. *Macromolecules* 1975, **8**, 552
20 Helfand, E. and Wasserman, Z. R. *Macromolecules* 1976, **9**, 879
21 Helfand, E. and Wasserman, Z. R. *Macromolecules* 1978, **11**, 960
22 Helfand, E. and Wasserman, Z. R. *Macromolecules* 1980, **13**, 994
23 Helfand, E. and Wasserman, Z. R. To appear in 'Developments in Block Copolymers' Ed. I. Goodman. Applied Science Publishers London, 1982
24 Leibler, L. *Macromolecules* 1980, **13**, 1602
25 Shen, M. and Kaelble, D. H. *J. Polym. Sci. Polym. Phys. Edn.* 1970, **8**, 149
26 Krause, G. and Rollmann, K. W. *J. Polym. Sci. Polym. Phys. Edn.* 1976, **14**, 1133
27 Chen, Y-D M. and Cohen, R. E. *J. Appl. Polym. Sci.* 1977, **21**, 629
28 Henderson, C. P. and Williams, M. C. *J. Polym. Sci. Polym. Lett. Edn.* 1979, **17**, 257
29 Diament, J., Soong, D. S. and Williams, M. C. In 'Contemporary Topics in Polymer Science' (Ed. W. J. Bailey) Plenum, New York, 1982 Vol 4
30 Djermouni, B. and Ache, H. J. *Macromolecules* 1980, **13**, 168
31 Leary, D. F. and Williams, M. C. *J. Polym. Sci., B* 1970, **8**, 335
32 Leary, D. F. and Williams, M. C. *J. Polym. Sci. Polym. Phys. Edn.* 1973, **11**, 345
33 Krause, S. *Macromolecules* 1978, **11**, 1288
34 Henderson, C. P. and Williams, M. C. Presented at IUPAC Macromolecular Symposium, Amherst, Massachusetts, 1982
35 Porod, G. *Kolloid-Z.* 1951, **124**, 83
36 Porod, G. *Kolloid-Z.* 1952, **125**, 51, 108
37 Ruland, W. *J. Appl. Crystallogr.* 1971, **4**, 70
38 Wiegand, W. and Ruland, W. *Prog. Colloid. Polym. Sci.* 1979, **66**, 355
39 Koberstein, J. T., Morra, B. and Stein, R. S. *J. Appl. Crystallogr.* 1980, **13**, 34
40 Koberstein, J. T. *J. Polym. Sci. Polym. Phys. Edn.* 1982, **20**, 593
41 Ruland, W. 'Colloque Franco-Americain sur la Diffusion des Rayons X et des Neutrons aux Petits Angles par les Polymeres', Strasbourg, September 1980
42 Worcester, D. L. Brookhaven Symposia in Biology 1975, No. 27, III, 37
43 Ghosh, R. E. 'A Computing Guide for Small-Angle Scattering Experiments' ILL Report No. 81GH29T
44 Roe, R. J. *J. Appl. Crystallogr.* 1982, **15**, 182